Climate Dynamics (2021) 57:2453–2466
https://doi.org/10.1007/s00382-021-05814-9

The impact of black carbon emissions from projected Arctic shipping on regional ice transport

Xueke Li[1] · Amanda H. Lynch[1,2] · David A. Bailey[3] · Scott R. Stephenson[4] · Siri Veland[5]

Received: 14 October 2020 / Accepted: 11 May 2021 / Published online: 18 May 2021

Abstract
The direct and indirect effects of global emissions of black carbon (BC) on the evolution of Arctic climate has been well documented. The significance of within-Arctic emissions of BC is less certain. In light of this, an ensemble of scenarios are developed that simulate the hypothetical diversion of 75% of current and projected shipping traffic from the Suez Canal to the Northern Sea Route (NSR). This experiment shows that BC from ships results in a small change in climate forcing that does not influence the Arctic-wide trajectory of change. However, the shift in forcing from the Suez route to the NSR not only influences regional evolution of sea ice cover, but also results in regional feedbacks that in some locations amplify (e.g. Greenland Sea) and in other locations damp (e.g. Labrador Sea) the sea ice retreat under anthropogenic climate change. The primary mechanism underlying these regional effects is a shift in circulation rather than direct thermodynamic forcing. The most significant impacts are distal from the emissions sources, which is likely to have policy implications as the expansion of industrial and transportation activities into the Arctic is considered.

Keywords Aerosols and particles · Ice · Earth system modeling · Climate change and variability · Arctic region

1 Introduction

Investors and communities alike are planning for the possible regime shift in Arctic shipping driven by receding ice, lower fuel prices, and industry consolidation (Duarte et al. 2012; Goldstein et al. 2018). This shift has the potential, as yet unrealized, to make the transpolar shipping route at least seasonally competitive with the Suez Canal (Buixadé Farré et al. 2014; Hansen et al. 2016; Meng et al. 2017; Ng et al. 2018; Theocharis et al. 2018), with attendant reductions in greenhouse gas emissions (Wang et al. 2020) or potential net warming due to joint effects of short-lived climate forcers in the short term (Fuglestvedt et al. 2014). Although the extent to which transit shipping along Arctic routes is economically viable remains under debate (Bekkers et al. 2018; Hildebrand and Brigham 2018; Lasserre 2014; Wan et al. 2018; Yumashev et al. 2017), ship traffic continues to increase due to Russian cabotage[1] (Gunnarson 2013), fish stock migrations, and increased tourism (Miller et al. 2020; Stewart et al. 2007).

Black carbon (hereinafter referred to as BC) emissions from the resulting increased ship traffic have been postulated to amplify Arctic sea ice retreat. Specifically, BC aerosols absorb strongly across visible and ultraviolet wavelengths. As a result, BC emissions can influence Arctic temperatures and the extent of ice and snow cover by (1) directly absorbing solar radiation (Flanner 2013; Stjern et al. 2017); (2) acting as nuclei to form cloud droplets and ice crystals, indirectly influencing cloud albedo via modifying the microphysical properties and lifetime of clouds (Haywood and Boucher 2000; Ramanathan and Carmichael 2008); and (3) reducing ice and snow albedo after deposition (Flanner et al. 2009; Ryan et al. 2018; Warren 1982). Previous studies

✉ Xueke Li
xueke_li@brown.edu

1 Institute at Brown for Environment and Society, Brown University, Providence, RI, USA

2 Department of Earth, Environmental and Planetary Sciences, Brown University, Providence, RI, USA

3 Climate and Global Dynamics Laboratory, National Center for Atmospheric Research, Boulder, CO, USA

4 RAND Corporation, Santa Monica, CA, USA

5 Department of Environment, Nordland Research Institute, PO Box 1490, 8049 Bodø, Norway

[1] Cabotage in this paper, following *Gunnarsson* (2013), is defined as domestic port-to-port transport by both domestic and foreign carriers.

suggest a measured decrease in Arctic albedo of 1.5–3.0% caused by snow and ice darkening from BC from all global combustion sources, onshore and offshore (Bond et al. 2013; Hansen and Nazarenko 2004).

Though BC aerosol plays an important role in the Arctic amplification of climate change, its interactions with the climate system and the consequent feedbacks are poorly constrained. For example, freshly emitted BC particles are generally hydrophobic and cannot serve as cloud condensation nuclei (CCN). Through microphysical aging processes, these carbonaceous particles gradually become hydrophilic on timescales that are highly variable (Fierce et al. 2015). These particles have a shorter average atmospheric residence time due to a high wet scavenging efficiency (von Schneidemesser et al. 2015). The uncertainty in atmospheric residence time of BC is particularly evident in estimates of the distance from ship stacks to deposition. Bond et al. (2013) suggest that BC has an overall positive radiative forcing, accounting for direct and indirect effects, of + 1.1 W m^{-2} globally with 90% uncertainty bounds of + 0.17 to + 2.1 W m^{-2}. The direct radiative effect, globally averaged of BC emission sources for the industrial era is estimated at + 0.71 W m^{-2} with 90% uncertainty bounds of + 0.08 to + 1.27 W m^{-2}. This estimate is derived from a number of highly uncertain processes, ranging from changes in albedo upon deposition, changes in snow metamorphism, phase partitioning in clouds, and cloud distribution properties.

Maritime transport utilizing heavy fuel oil (HFO) contributes to BC emissions in the Arctic via incomplete combustion (Corbett et al. 2010; Wu et al. 2018). Unlike BC transported to the Arctic from sub-Arctic terrestrial sources, BC emitted in the Arctic is more likely to remain at low altitudes, due to the typically strong surface inversion, particularly in the winter months. It has been posited that this has the potential to cause Arctic surface temperature to be nearly five times more sensitive to BC emitted within the Arctic than to emissions from lower latitudes, even though these emissions are much smaller in magnitude (Sand et al. 2013a, 2016). It is unclear, however, how the frequency of surface inversions will change in the coming century (Medeiros et al. 2011).

As a result of this potentially high sensitivity, studies have considered whether BC emissions from Arctic shipping could amplify or damp sea ice extent and snow cover feedbacks. Amplification of snow- and ice-albedo feedbacks can occur by deposition, lowering the high albedo of ice and snow (Browse et al. 2013; Corbett et al. 2010; Ødemark et al. 2012; Sand et al. 2016). Damped feedback of BC emissions can occur through direct aerosol effect or indirect effects on clouds; for example, Fuglestvedt et al. (2014) observed a decrease in the net direct effect of BC when shifting shipping to the Arctic. Stephenson et al. (2018) find an increase in the formation of clouds with high liquid water content could cause cooling relative to the shipping-free Arctic. All of these studies come with the caveat that BC emissions from Arctic shipping are small compared to those from the terrestrial sub-Arctic, such that the climatic impact of BC emitted from Arctic shipping is likely to be overshadowed by that emitted from terrestrial sources. BC emissions from Arctic shipping may be reduced further in the context of a switch from HFO to low-sulfur diesel fuel or liquefied natural gas (LNG), as well as the reduced need for icebreakers, but the significance of ship-sourced BC may increase as emissions from industry are reduced. Adding complexity to this issue, some blends of low-sulphur fuels combusted at low engine loads have been linked to a possible 85% increase in BC emissions (DNV 2020). Appropriate regulation of BC emissions from Arctic shipping traffic has been characterized as providing a "quick win" for shipping companies through the use of relatively inexpensive scrubbing technology, making a focus of BC effects alone a policy relevant target for enquiry, even though other shipping emission pollutants such as sulfates may exert more significant climatic effects over the Arctic (Baker et al. 2015; Fuglestvedt et al. 2014; Stephenson et al. 2018). In this context, then, we are seeking to understand the additional forcing of Arctic shipping-related BC, and in particular whether it constitutes a feedback of significance in the evolving Arctic system.

2 Data and methods

2.1 Climate model configuration

To quantify climate feedbacks of BC, we use the newly released Community Earth System Model version 2 (CESM2) at approximately 1° horizontal resolution with 32 vertical layers for the atmospheric component. CESM2 is a fully coupled earth system model that provides state-of-the-art simulations of climate. It contains seven prognostic model components (CAM6/WACCM6, CLM5, CISM2, POP2, CICE5, MOSART, and WW3) to comprehensively represent interactions among atmosphere, land, land-ice, ocean, and sea ice (Danabasoglu et al. 2020).

The atmospheric component CAM6 improves upon its previous version by including a unified turbulence scheme (Golaz et al. 2002), adopting an updated Morrison-Gettelman cloud microphysics scheme (MG2) (Gettelman and Morrison 2015), and applying a new scheme to calculate subgrid orographic drag (Beljaars et al. 2004). Notably, CAM6 treats aerosols using a four-mode version of Modal Aerosol Model (MAM4) (Liu et al. 2016). That is, apart from Aitken, accumulation, and coarse modes preserved in the three-mode version (MAM3) (Liu et al. 2012), an additional primary carbon mode is included in MAM4 to reside freshly emitted particulate organic matter (POM)

and BC particles. This strategy allows for the conversion of particles from hydrophobic to hydrophilic. Compared to simulations with MAM3 that combine the primary carbon mode with the accumulation mode, which as a consequence, enhances wet removal of BC, the treatment of separating the primary carbon mode from the accumulation mode in MAM4 enhances seasonal variation of near-surface BC concentrations and increases near-surface BC concentrations in the polar regions by a factor as large as 10 (Liu et al. 2016).

The sea ice model specified in CESM2 is the Los Alamos sea ice model version 5.1.2 (CICE5, Hunke et al. 2015) and is described in detail in Bailey et al. (2020). It has a uniform horizontal resolution of 1.125° zonally and varies from 0.38° to 0.64° meridionally in the Arctic (DuVivier et al. 2020). CICE5 is an improvement over the previous version in that it adopts a new mushy-layer thermodynamics to represent prognostic salinity structure (Bailey et al. 2020; Turner and Hunke 2015) and leverages a new level-ice melt pond framework to simulate melt pond processes (Hunke et al. 2013). The vertical layers of ice and snow have been upgraded to eight and three, respectively, to better capture the vertical profiles of salinity and temperature. Relevant to this study, the sea ice component contains a multiple-scattering radiation scheme known as the delta-Eddington formulation (Briegleb and Light 2007), which computes the absorbed shortwave and resulting albedos for the snow-covered, pond-covered, and bare ice fractions of the cell, separately. In CICE5, three types of aerosols are activated. They are hydrophobic BC, hydrophilic BC, and a single kind of dust (Holland et al. 2012). Aerosols deposited on ice and snow are treated as volume-weighted tracers. Each aerosol species is assigned two tracers: one resides in the surface scattering layer (SSL) and the other in the snow or ice, which is beneath the SSL. The lifecycle of tracers follows that once the upper layer (SSL or snow/ice interior) is vanished due to surface melting, tracers will either flow to the layer underneath or disappear in the ocean when there is no ice to hold up. The scheme allows aerosols such as BC—a radiatively active tracer—to be carried around on the sea ice as well as migrate vertically as the snow and sea ice change. The thermodynamics of aerosol change can be resolved from the diagnostic variables (Hunke et al. 2015). The impacts of BC in the CESM1 sea ice were assessed in Holland et al. (2012) and were found to have a generally small local effect on the thermodynamics.

In addition, the CESM large ensemble (CESM1-LENS, Kay et al. 2015) is used as a kind of proxy testbed (Deser et al. 2020) to provide a more nuanced assessment of uncertainties arising from internal variability. The Large Ensemble Project provides 40 ensemble members performed with 1° resolution of fully-coupled CESM1 under RCP 8.5 from 2006 to 2100. As is standard practice, the slightly varying initial condition leads to an ensemble spread solely due to the model's internal climate variability (Kay et al. 2015). While this is not the model implementation used here, this same feedback gain calculation is also performed with the not-yet-published CESM2 large ensemble (CESM2-LE; detailed at https://www.cesm.ucar.edu/projects/community-projects/LENS2/). Taken together, they can provide guidance as to the spread that might be expected in model responses in the present application. It should be noted that at the time of submission, all of the required variables from the CESM2 implementation of this large ensemble were not available.

2.2 Shipping emissions scenarios

Two sets of climate simulations with the CESM2 from 2015 to 2065 are performed. In both sets, projected monthly BC emissions from simulated trans-Arctic voyages are injected into the atmosphere along with BC emissions from Peters et al. (2011) and other emissions inventories from IPCC AR5 (Lamarque et al. 2010) based on the Shared Socioeconomic Pathway (SSP) 5 under the Representative Concentration Pathway (RCP) 8.5 scenario (O'Neill et al. 2016, hereinafter referred to as SSP5-8.5). BC emitted from Arctic shipping is injected in the primary carbon mode of CAM6. Specific modifications of the control experiment and the rationale to develop perturbation experiments are outlined below.

Small errors in the existing CMIP6 SSP5-8.5 scenario forcing (Fig. 1a) were corrected to create a new control experiment rather than using the standard CMIP6 scenario. The main issues with the original SSP5-8.5 data are as follows. First, BC emissions in the standard scenario assume that the NSR is navigable all year round regardless of ice cover, when in reality, Arctic voyages are heavily concentrated in the peak months of July through October. We therefore limited shipping emissions to those months in which the NSR was technically accessible following the method of Stephenson et al. (2018), in order to reflect the seasonal cycle of Arctic shipping traffic. Second, there are interpolation artifacts in the standard scenario that are evident year round near the North Pole, which we have termed the "Santa Claus effect"; these were removed. Third, the HFO ban was implemented from 2020 in the standard scenario, but it is not yet in force. In November 2020, the IMO approved a recommendation to ban the use and carriage of HFO in the Arctic by July 1, 2029 for Arctic country-flagged vessels operating in domestic waters, and by July 1, 2024 for all other voyages (Humpert 2020; Reuters Staff 2020). Nevertheless, in the SSP5-8.5 forcing, the BC emissions are assumed to rise until 2020 and then begin to drop after this point, likely due to other treaties and not related to the HFO ban (O'Neill et al. 2014). To address this complexity, the BC emissions in the new control simulation are modified as shown in Fig. 1b and the difference map after correction is shown in Fig. 1d.

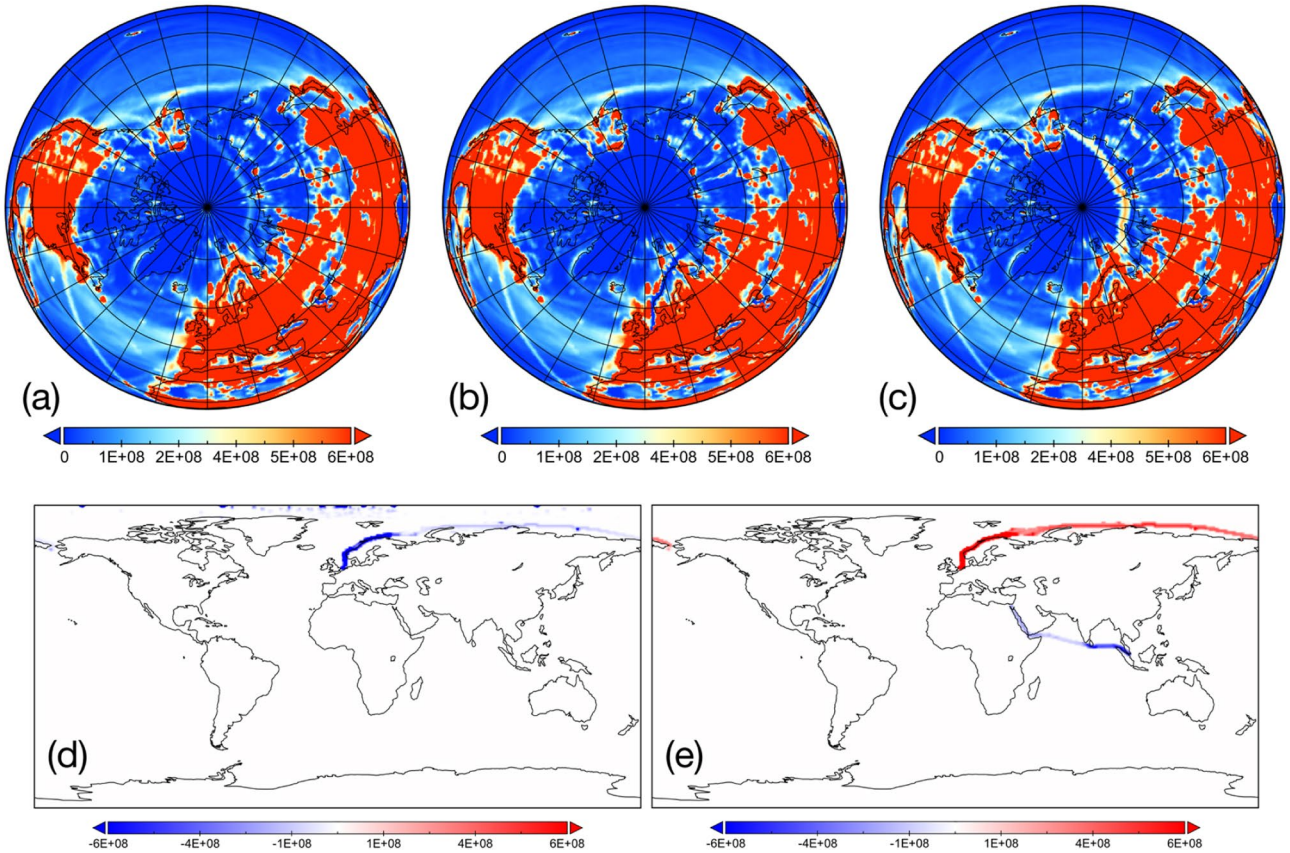

Fig. 1 Global maps of BC anthropogenic emissions (unit: molecules/cm^2/s) in February 2050 for **a** the standard SSP5-8.5 scenario forcing, **b** our modified forcing for the control simulation, **c** the emissions associated with the "big kick" ensemble, **d** difference between modified and standard SSP5-8.5 scenario forcing, calculated as **b** − **a**, and **e** difference between the "big kick" experiment and the control simulation, calculated as **c** − **b**. Time series of averaged BC emissions along the NSR for the standard CMIP6 SSP5-8.5, control and "big kick" experiments are provided in Figure S1 in supplementary material

To summarize, the aspects of the standard SSP5-8.5 forcing modified in the control include: (1) BC emissions for the technically non-navigable months; (2) spurious BC emissions near the North Pole; and (3) declining BC emissions after the year 2020. Notably, while BC emissions show an increasing trend over time, sea ice concentration and snow covered on ice decrease with time (Figure S2 in supplementary material). Therefore, ice and snow albedo response is likely weakened due to the presence of melt ponds towards the end of the simulation, which is also corroborated by Bond et al. (2013) and Holland et al. (2012).

With the recent fall in oil prices, reasons to utilize the NSR for transit shipping have been less compelling in the near term. International transit shipping utilizing the entire NSR comprised less than 1% of all voyages from 2016 to 2018 (B. Gunnarson, personal communication, 2020). These transits were primarily associated with demonstration voyages and the repositioning of vessels. In contrast, cabotage along the Russian Arctic coast comprised 88% of the total Arctic voyages on average over the same period, with monthly peaks of at least 250 voyages from July to October, and up to 400 voyages in September in some years (B. Gunnarson, personal communication, 2020). Thus, emissions associated with NSR transit shipping are a small fraction of the total BC load associated with Arctic shipping at present. Furthermore, the BC load in the Arctic is comprised primarily of sub-Arctic terrestrial sources (Law and Stohl 2007; Shindell et al. 2008). In this uncertain context, to unambiguously characterize the climatic response to a postulated highly active route, a large perturbation was designed. The experiment is thus designated "big kick". Specifically, this approach lays the groundwork for understanding better what useful information might be gleaned from climate simulations of the impacts of NSR shipping in general, and where greater precision is likely to be most effective. In that spirit, an ensemble of integrations is conducted that re-routes 75% of BC emissions from current and projected Suez Canal traffic (Gidden et al. 2019) during 2015–2065 to the Arctic, at equal 0.5° intervals along a route from the Bering Strait to Rotterdam (Fig. 1c). Other settings are the same as the control except that ship voyages may occur year-round

to reflect a large perturbation. That said, the major differences between the control and perturbation experiments are: (1) 75% diversion of BC emissions from the Suez Canal route to the NSR; (2) BC emissions from the modified CMIP6 SSP5-8.5 scenario for the technically non-navigable months (Fig. 1e). Each of the ensemble members was performed with the "big kick" emissions, and a small perturbation to the surface air temperature to create internal variability. While four ensemble members is small, this should be sufficient to detect a signal in atmospheric circulation and sea ice responses, as described in Deser et al. (2012). Furthermore, we justify this sufficiency through an analysis of the signal to noise ratio of the first four empirical orthogonal functions (EOFs) based on Shepherd (2014) and Chen et al. (2019). The results are detailed in Figure S3 in supplementary material.

2.3 Quantifying feedback gain

The "big kick" experiments introduce an additional BC load to the business-as-usual scenario (the control simulation). This permits an understanding of the potential for BC load to amplify or damp greenhouse gas feedback effects, as opposed to only quantifying the additional forcing (both positive and negative) that BC imposes on the system. BC could both amplify (through albedo reduction, Hansen and Nazarenko 2004) and damp (through increases in cloud liquid water content, Stephenson et al. 2018) the Arctic response to climate change. This is addressed through a feedback gain calculation following Dufresne and Bony (2008) based on the simple planetary energy balance response to a change in radiative forcing ΔR, viz.,

$$\Delta T = \frac{\Delta F^{rad}_{TOA} - \Delta R}{\lambda} \tag{1}$$

The total feedback effect can be divided into:

$$\lambda = \lambda_0 + \lambda_w + \lambda_{LR} + \lambda_c + \lambda_\alpha \tag{2}$$

where λ_0, λ_w, λ_{LR}, λ_c, and λ_α are feedback parameters of Planck, water vapor, lapse rate, cloud, and albedo, respectively. To this set, we add a BC feedback parameter. Using this we can compare the basic equilibrium response (ΔT_E) to the observed temperature response (ΔT), for example, by defining a feedback gain variable g, given by:

$$\Delta T = \frac{1}{1-g}\Delta T_E \tag{3}$$

in which $g = \sum_{x\neq 0} g_x$, and $g_x = -\frac{\lambda_x}{\lambda_0}$. Thus, we can calculate the feedback gain due to the change in BC forcing between the control and "big kick" experiments (termed as g_{BC}) by

$$\Delta T_{65-15,"bigkick"} = \frac{1}{1-g_{BC}}\Delta T_{65-15,control} \tag{4}$$

where the subscripts "65" and "15" represent annual mean value in the year 2065 and 2015, respectively.

A similar procedure can be followed for ice volume and area. We primarily focus on the sea ice response since changes in BC burdens are more pronounced and significant over sea ice than land (Figure S4 in supplementary material). We acknowledge that our experiments are not in equilibrium, but nevertheless this is a useful measure that allows the integration of multiple interacting effects into a single metric. This serves to direct attention to more detailed analysis.

For analysis of the whole Arctic Ocean and its subregions, we define the Arctic following Parkinson and Cavalieri (2008) (thumbnail image shown in Fig. 3a) with constituent sub-regions demarcating the Labrador Sea, the Greenland Sea, the Barents and Kara Seas, the Siberian Sea, the Beaufort Sea, the Central Arctic, the Arctic Ocean (including the Siberian Sea, the Beaufort Sea, and the Central Arctic, not shown), the Bering Sea, Seas of Okhotsk, the Canadian Arctic Archipelago, and Hudson Bay, abbreviated as Lab, GIN, Bar, Sib, Beau, CArc, ArcOc, Bering, Okhotsk, CAArch, and Hudson, respectively. To better illustrate the magnitude of the BC emission perturbation, seasonal total BC emission burden across the whole Arctic and in the abovementioned Arctic sub-regions in the standard CMIP6 SSP5-8.5 scenario, control and "big kick" experiments are shown in Table S1 in supplementary material.

3 Whole Arctic response

The total response to BC over the whole Arctic—ice volume, concentration, and distribution, surface temperature, broadband albedo, cloud fraction, longwave and shortwave heating rates—is modest, in line with previous studies (Flanner 2013; Holland et al. 2012; Sand et al. 2013b). These are not shown, since the significant differences (even at the 90% significance level) are very small. An indication of these differences is summarized in Table 1, in the form of linear trends for the last thirty years of the integrations (2035–2065) for the control experiment and the "big kick" ensemble mean. Based on these trends, it could be argued that the ice volume across the whole Arctic diminishes slightly more rapidly and the temperature increases slightly more in the ensemble mean compared to the control, as the presence of additional BC load in the Arctic atmosphere does result in the expected physical responses. But as is readily apparent, in the context of high interannual variability in this system, these results in aggregate are not statistically significant. More detail can be seen for example in Fig. 2, which shows the time series of ice volume differences from each season, averaged across the

Table 1 Arctic wide average linear trend, per decade, 2035–2065, showing results from the control simulation, the perturbation ensemble mean and the standard deviation of the ensemble (in brackets)

	Season			
	DJF	MAM	JJA	SON
Ice volume (m/decade)				
Control	− 0.008	− 0.008	− 0.008	− 0.004
"Big Kick"	− 0.010 (0.003)	− 0.009 (0.002)	− 0.008 (0.002)	− 0.005 (0.001)
Ice area (/decade)				
Control	− 0.297	− 0.106	− 0.373	− 0.515
"Big Kick"	− 0.358 (0.140)	− 0.075 (0.070)	− 0.383 (0.110)	− 0.559 (0.119)
Albedo (/decade)				
Control	− 0.001	0	0	− 0.001
"Big Kick"	− 0.001 (0)	0 (0.0005)	0 (0)	0 (0.0005)
Surface temperature (K/decade)				
Control	0.125	0.052	0.041	0.085
"Big Kick"	0.156 (0.049)	0.058 (0.020)	0.043 (0.009)	0.088 (0.020)

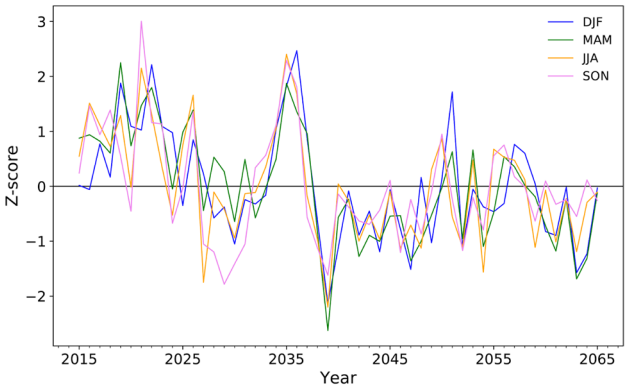

Fig. 2 Time series of ice volume difference between the "big kick" ensemble mean and the control simulation over the Arctic, expressed as a Z-score. The Z-score (z) measures the divergence of a given value x to the mean of the sample (μ) in the unit of standard deviation (σ). It can be expressed by the formula: $z = \frac{x-\mu}{\sigma}$. A Z-score of 0 indicates the value is identical to the mean while that of -1 and 1 indicates the value is one standard deviation below or above the mean, respectively

ensemble members, expressed as a Z-score. This behavior is quite representative of individual ensemble member results in every season, and of other measures such as surface temperature and longwave heating rate. As is readily apparent, on an Arctic-wide basis, the rate of ice loss does not accelerate in the "big kick" experiment ensemble relative to the control. Thus, it is apparent that there is no net amplification (nor a damping) of the response that is sufficient to set up an additional feedback in the whole Arctic system.

This conclusion is reflected most efficiently in the calculation of the feedback gain parameter. In order to set bounds for significance in the feedback gain parameter, the CESM1-LENS ensemble members were compared pairwise (Fig. 3a). The gain calculation is shown for the entire Arctic at the left of the figure, as well as being disaggregated into each of the Arctic Seas. The median feedback for the whole Arctic is 0.00 with standard deviation of 0.21 for surface temperature, 0.21 for ice concentration and 0.20 for ice volume. The shading corresponds to the probability that the feedback gain magnitude would have been evident through internal system variability alone. This figure shows the potential for large feedback gain values evident particularly in the Barents and Bering Seas generated by internal variability in the ensemble. Bringing the focus to the range more typical of the experiments being assessed here (Fig. 3b) shows that—for the whole Arctic—the feedback gain in the "big kick" experiment cannot be considered to be significant for surface temperature, aggregate ice concentration or ice volume per unit area. As a result, it can be concluded that this experiment confirms previous research indicating that Arctic shipping, while having the potential to perhaps slightly influence the trajectory of Arctic sea ice retreat, does not induce additional Arctic-wide feedbacks.

4 Regional response

The same cannot be said, however, when disaggregating the response. Figure 3 also shows the feedback gain parameter for 11 distinct regions of the Arctic. The median feedback gain for the CESM1-LENS is zero for each of these regions. It is apparent that feedbacks are generated in the "big kick" ensemble in some of these regions at levels that amply exceed one standard deviation in the CESM1-LENS. This is corroborated by the feedbacks produced by the CESM2-LE (not shown), exhibiting significant difference in the GIN Seas, Barents/Kara Seas, and Bering Sea. While this cannot be a strict test of statistical significance, because of the different model configurations, it can serve as a guide to model responses that are likely to be outside of expectation from random chance.

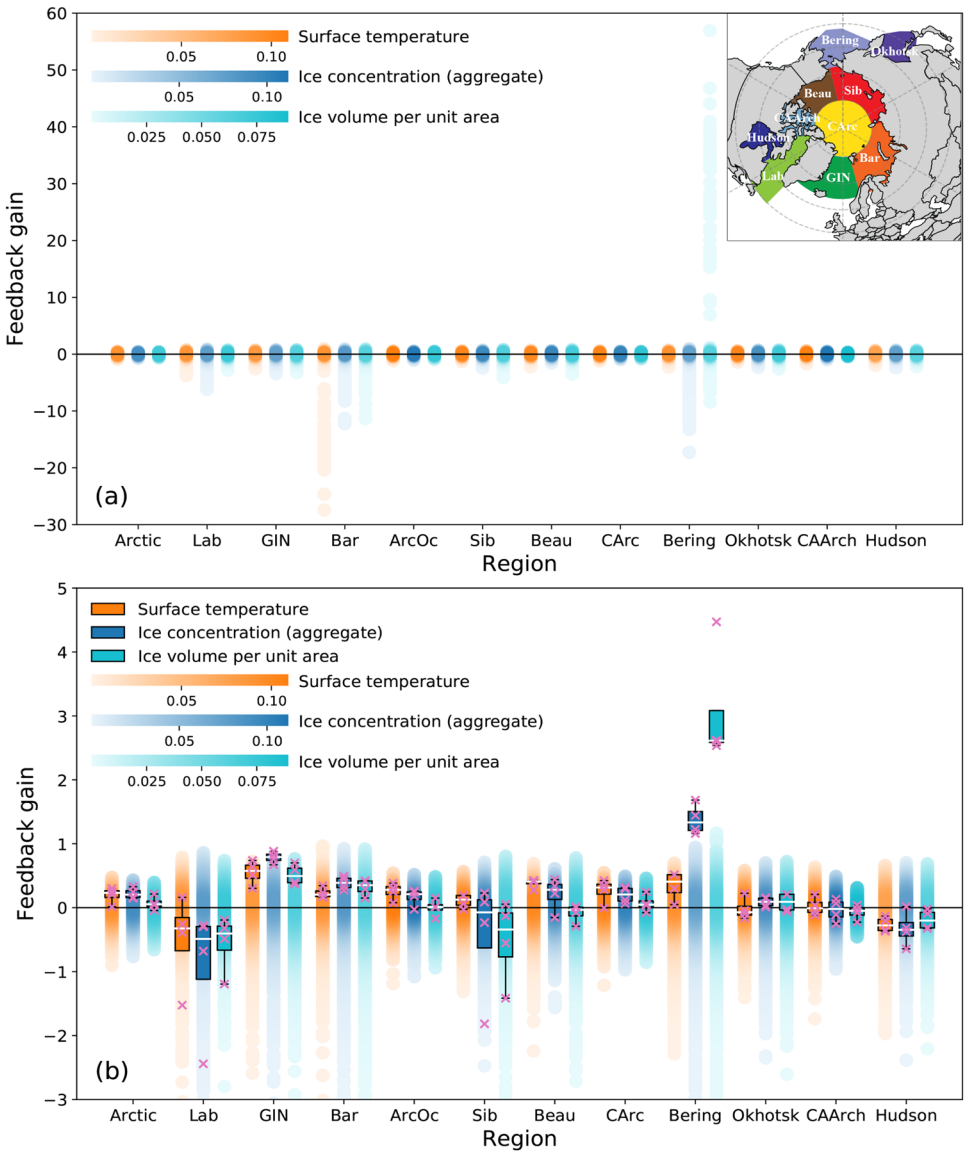

Fig. 3 Response of BC in the Arctic and each subregion as defined by Parkinson and Cavalieri (2008) showing **a** the feedback gain parameter (unitless) of the CESM1-LENS ensemble members selected pairwise (and a thumbnail map of the regions), and **b** a comparison of feedback gain parameter between the CESM1-LENS ensemble members (same as **a**, but with constrained range) and the "big kick" experiments (that is, g_{BC}, shown in pink cross mark). Shading of the CESM1-LENS results (unitless) indicates the frequency of feedback gain value inferred from the probability density function, with darker colors implying higher frequency. The boxplot displays the median (white line) and interquartile range (IQR, black box) whiskers across four ensemble members of the "big kick" experiment. The IQR encompasses from 25th percentile (Q1) to 75th percentile (Q3). The upper and lower whiskers are bounds of Q3 + 1.5*IQR and Q1-1.5*IQR, respectively

The larger feedback gain values (mostly for the ice parameters) are negative in Baffin Bay and the Labrador and Siberian Seas, strongly positive in the Bering Sea, and somewhat positive in the GIN Seas and to a lesser extent the Barents/Kara Seas. The differing signs of the feedback gain in different regions suggest why the Arctic-wide feedback is effectively zero. That said, even though the median is zero, the variance in internally generated feedback gain in the CESM1-LENS is substantially greater than one in the Bering and Barents/Kara Seas, and as a result these two regions will be largely excluded from the following discussion.

It is particularly meaningful from a policy standpoint that the regions showing the largest "significant" feedback responses are distant from the regions where the additional BC load of the "big kick" experiment is largest (Fig. 1). That said, practical regulatory policies can be targeted at urgent priority areas by leveraging the "remote climate impact". Furthermore, this regional response suggests that the ice changes are influenced, if not driven, by perturbations in ice and atmosphere dynamical effects rather than albedo forcing by proximal deposition, or local cloud radiative forcing. This is borne out by, for example, a comparison of the longwave and shortwave heating rates in the GIN Seas (Figure S5 in supplementary material). Thus, the postulated mechanism is efficient upward transport of BC relative to other aerosols (Liu et al. 2020), with spring (MAM) in particular, leading to changed patterns of heating aloft, causing a perturbed atmospheric circulation that re-distributes ice distant from the emitted BC and subsequent distal thermodynamic responses. Evidence supporting this mechanism is provided in the following.

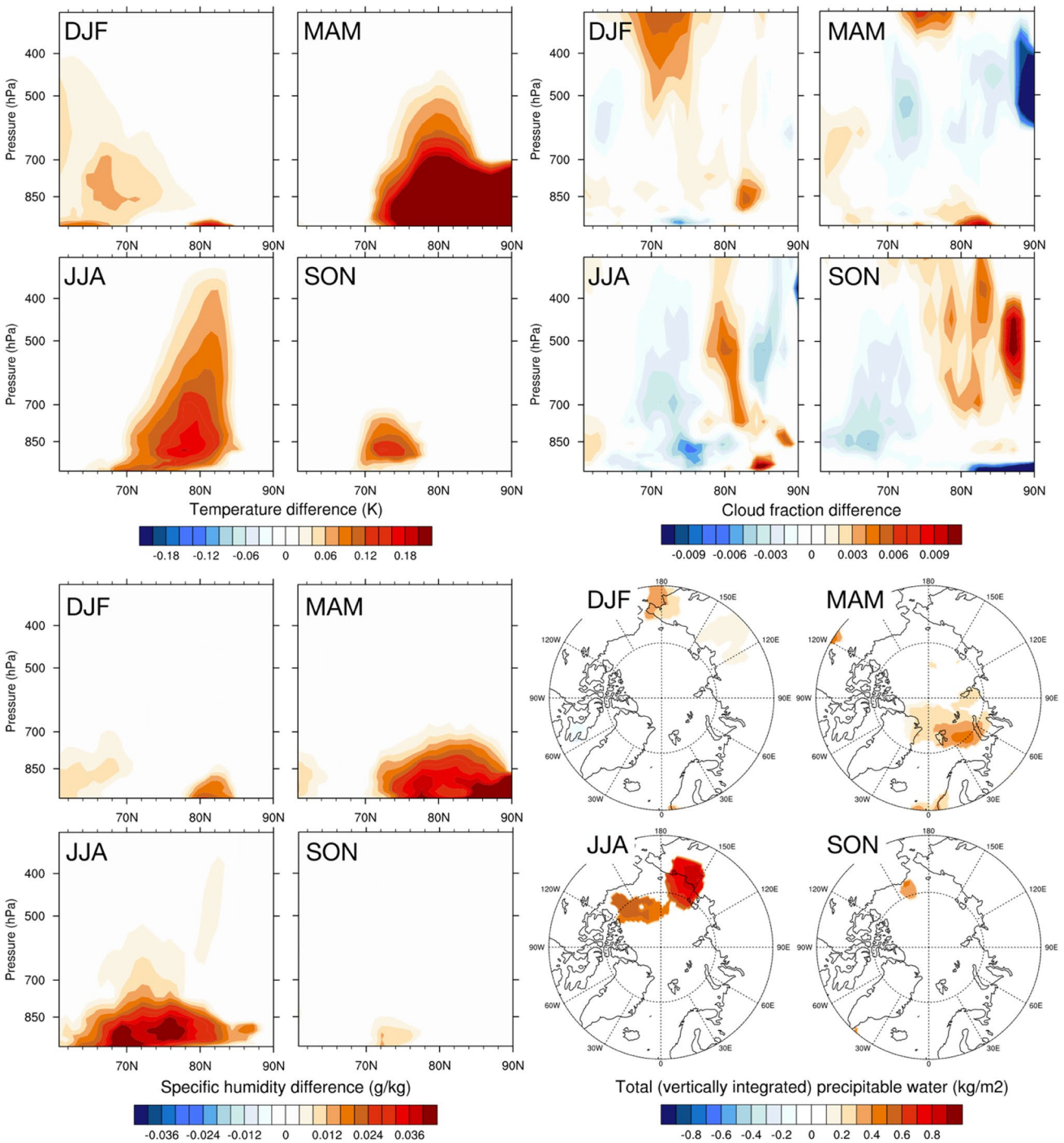

Fig. 4 Seasonal difference in temperature, cloud fraction, specific humidity, and total precipitable water between "big kick" ensemble mean and control from 2035 to 2065. The first three variables are shown as zonal average profiles whereas the last variable is displayed at the surface level. Only values significant at the 90% level are shown

The associated atmospheric heating exhibits distinct altitude-dependent features (Fig. 4), including increased cloud cover and precipitation at low altitudes but decreased cloud and precipitation at high altitudes (consistent with Ban-Weiss et al. 2012; Johnson et al. 2019). During winter, the absence of solar radiation creates a temperature inversion, acting as a cap that prevents the upward motion of BC. In contrast, insolation in spring and peaking in summer destabilize the vertical temperature profile, resulting in larger dynamical responses in those seasons.

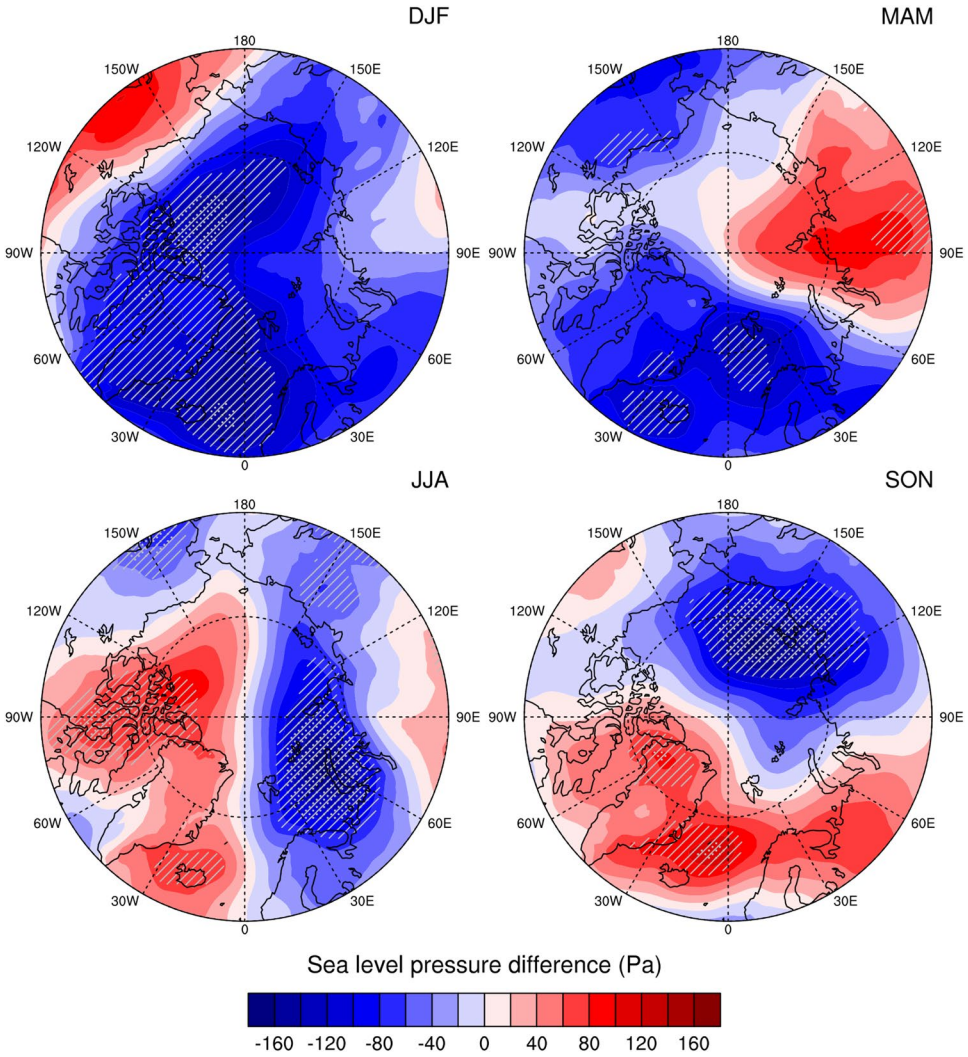

Fig. 5 Difference of sea level pressure between "big kick" ensemble mean and control for each season, defined by the months indicated, for the period 2035–2065, stippled where the difference is significant at the 90% level and hatched where the difference is significant at the 80% level

The sea level pressure (SLP) changes provide a useful indicator of these atmospheric dynamical responses (Fig. 5). The changes are modest but systematic, and may be summarized as a small but consistent tendency toward less negative indices for both the Northern Annular Mode and the Arctic dipole patterns (which can be diagnosed, for example, from the loadings onto EOF1 and 2 in the 1000 hPa height fields, but are also apparent in the SLP patterns). This effect is in the context of an enhancement in the propensity toward a negative index Northern Annular Mode associated with greenhouse gas emissions that is typical of most climate change scenarios (Gillett and Fyfe 2013). These small shifts in the circulation that act as a perturbation on greenhouse gas forcing result in a reduction in the transpolar drift stream, a weakening of ice evacuation from the Siberian coast toward the Beaufort Sea, and a weakening of the ice exported out through the Bering Strait (Figure S6 in supplementary material). All of these effects are consistent with the negative feedback gain parameter in the Siberian Sea and with findings such as those of Wang et al. (2009). This is also consistent with the small but positive feedback gain in the aggregate ice area in the Beaufort Sea.

In the spring (MAM), there is also an eastward shift of the Siberian high associated with the Arctic Dipole (AD) in the ensemble mean "big kick" experiment (Fig. 5). While the loading onto the AD mode varies across ensemble members, all members show an increasing propensity toward a positive mode in the last 2 decades of the simulations. This shift towards a slightly positive phase of AD has been demonstrated to lead to favorable conditions for enhanced ice export toward the Atlantic (Watanabe et al. 2006).

In the summer (JJA), the SLP difference between the ensemble mean and the control reveals positive values centered on the western Arctic (that is, Iceland-Greenland-Canadian Arctic Archipelago-Beaufort Sea) and negative values centered on the eastern Arctic (Barents and Kara Seas-Laptev Sea-Siberian Sea). This feature is also evident in the results of Overland et al. (2012). This persistent AD

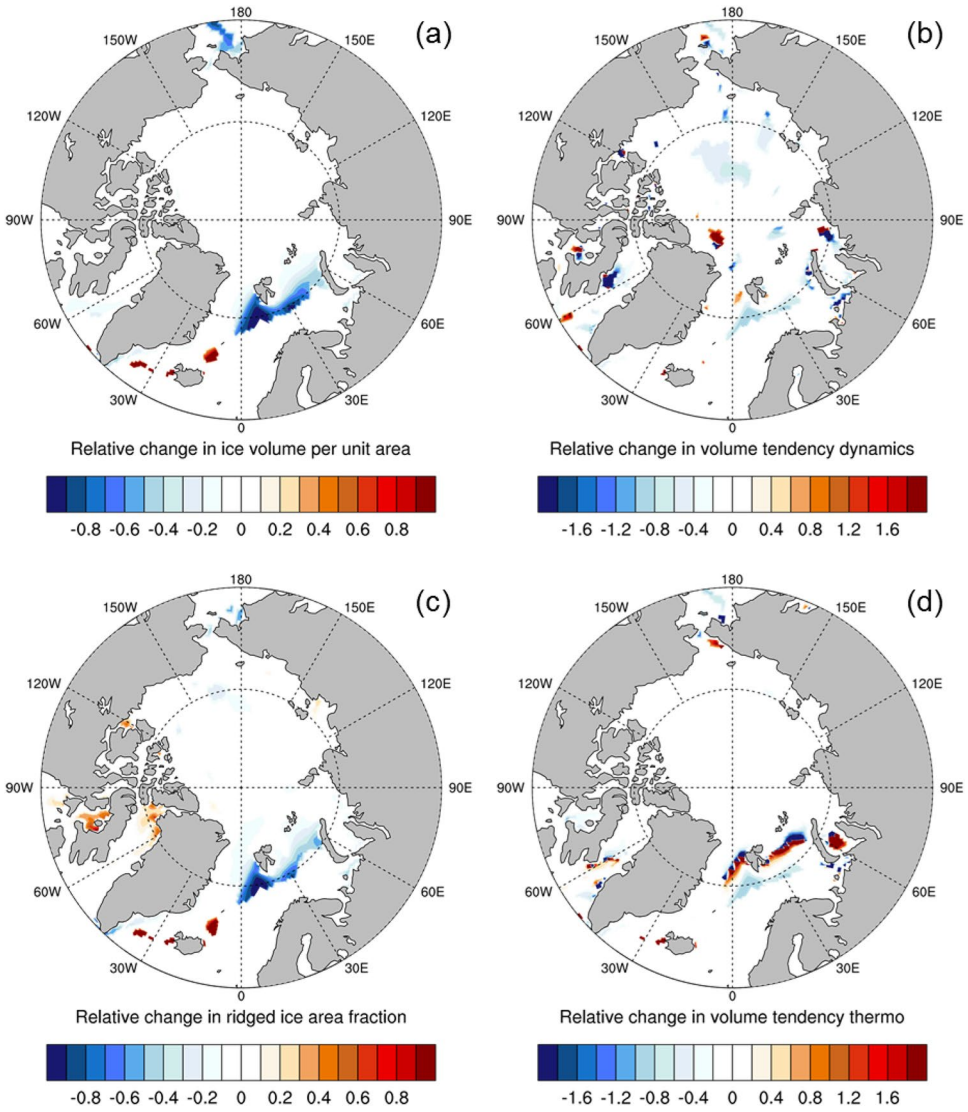

Fig. 6 Relative change in spring ice volume between "big kick" ensemble member 1 and control 2035–2065 by **a** total, **b** dynamic, **c** ridged and **d** thermodynamic processes. The relative change is computed using $(\text{Value}_{\text{"big kick"}} - \text{Value}_{\text{control}})/\text{Value}_{\text{control}}$. Only values significant at the 90% confidence interval are shown

signature facilitates southerly wind flow from the Bering Strait, bringing warm North Pacific waters into the Arctic Ocean, but also accelerating ice export through Fram Strait (Wang et al. 2009).

The signal in the North Atlantic is stronger, whereby the deepening of the polar low storm track in the GIN Seas is apparent, in all seasons, but particularly winter (DJF) and spring (MAM) (Fig. 5). The impact on the ice regime in MAM is shown in Fig. 6 for total, dynamic, ridging and thermodynamic ice differences from "big kick" ensemble member 1 for enhanced clarity (with the total MAM ice volume change for the other ensemble members shown in Figure S7 in supplementary material). The overall impact in ice volume shows a redistribution from the eastern Barents and Kara Seas to the marginal ice zone in the GIN Seas. This is as a result particularly of the influence of dynamical processes as shown in the difference in ice volume due to ice transport and ridging (Fig. 6b and c), although this is also reflected somewhat in the distribution of ice growth and melt (Fig. 6d). An enhancement of the polar low storm track in all seasons apart from summer (JJA) leads to an increase in the incursion of sub-Arctic air into the region, with concomitant warming in the GIN and Barents Seas. Consistent with this logic are ice velocities that are generally more cyclonic in this region in the "big kick" ensemble members and increased ice drift speed in the region of enhanced export. As a result, significant changes in the ice regime are manifest all along the eastern Greenland coast even though this is distal from the perturbation in shipping activity.

The negative feedback gain parameters in the Baffin Bay and Labrador Sea region are also driven primarily by ice transport effects. This region, typical of Arctic projections, maintains a relatively heavy seasonal ice cover throughout much of the simulation across seasons, with spring (MAM) ice concentrations relatively flat at around 60% throughout the entire integration, even as the region is close to ice free

in fall (SON). Ice thickness decreases in every season, and most rapidly in winter (DJF) and spring (MAM). Consistent signals across all ensemble members yielding statistically significant differences are also evident in warming temperatures and increased ice export from Baffin Bay out through the Labrador Sea (Figure S6 in supplementary material). These changes in ice regime are then reflected in an increase in ice associated with thermodynamic growth. The conclusion based on these observations is that the modest additional warming evident in the "big kick" experiment is insufficient to offset the increased growth in ice as the shift in ice drift evacuates ice toward the south. A negative feedback then results in the western Greenland coastal zone.

This kind of integrative impact on ice cover associated with subtle shifts in circulation has been documented by Kwok (2000), Maslanik et al. (2000) and Rigor et al. (2002). These dynamical mechanisms may also have profound implications for weather extremes in the mid-latitude (Cohen et al. 2014; Coumou et al. 2018).

5 Discussion

The future significance of international transit shipping in the Northern Sea Route will depend on numerous factors, including the interests and aspirations of Arctic nations, a sustainable cargo base, the length of the navigation season, and the availability of navigational support services and infrastructure. In this context, the effects of shipping on the climate system of the Arctic are small, but in our view, not insignificant.

The mitigation of black carbon emissions was expected to present "a potentially valuable opportunity with a very short delay between action and effect" (Grieshop et al. 2009, p. 533). This is particularly true for the Arctic due to the short time from emission to deposition [days to weeks (Bond et al. 2013; Hansen and Nazarenko 2004)]. Our findings suggest this opportunity is more limited than might have been hoped. It is evident from these experiments and analyses that even a large perturbation in the usage of the Northern Sea Route, with its concomitant increase in black carbon emissions, is unlikely to be a significant factor in accelerating Arctic sea ice loss. Although statistically significant surface warming adjacent to sea ice loss regions is detected (Figure S8 in supplementary material), as evidenced by Screen et al. (2014), the magnitude is small and does not result in an amplification of greenhouse gas associated warming. It should be noted that by design, these simulations did not include the impacts of sulfate aerosols that attend enhancing shipping emissions, which can often yield a cooling effect (Stephenson et al. 2018). Further work is required to understand the relative importance of other shipping emission pollutants such as sulfate and organic carbon under varying shipping scenarios. What is significant, however, is that these emissions do have the potential to affect regional feedback processes, that the mechanism underlying these effects is largely dynamical changes in the system, and that the most significant impacts are distal from the emissions themselves. Importantly, it appears that a response is via the North Atlantic storm track, which has significance for operations in this busy region of the Arctic. As a result, policy-makers may have an interest in knowing more precisely what level of black carbon load, regardless of source, induces the observed regional changes.

In the evolving Arctic transportation policy context, it is critical to disentangle the underlying physical mechanism that links BC emissions to the potentially integrative effects on atmospheric circulation. Our results suggest that BC emissions affect the circulation primarily through the propagation of the small perturbation via a convective pathway. The subsequent dynamic response then plays an important role in regional impacts. A case in point is a weakening and poleward shift of mid-latitude storm tracks that is disproportionate to the global BC forcing (Johnson et al. 2019).

Furthermore, the future of emissions contributions from Arctic ships—be they engaged in fishing, cabotage or transit—depends on the speed of technological developments and adoptions toward zero-emission fuels. The International Maritime Organization aims to halve emissions from shipping by 2050, while Arctic nations may adopt more ambitious targets in their sovereign seas. For example, the Norwegian Shipowners' Association has stated a goal of halving emissions by 2030, and to purchase only ships with zero-emissions technology from 2030. While these are relatively minor goals in the global black carbon budget, such aspirations form an important part of an overarching maritime shipping strategy.

Supplementary Information The online version contains supplementary material available at https://doi.org/10.1007/s00382-021-05814-9.

Acknowledgements This research was funded by the National Science Foundation through Grant NNA/CNH-S 1824829: Modeling risk from variation in a coupled natural-human system at the Arctic ice edge. The authors appreciate the insightful discussions with Michael Goldstein on the motivations for and relevance of these simulations for policy and communities. There are no conflicts of interest to report for any authors on this paper, not for the colleagues we acknowledge here. Previous and current CESM versions are freely available at www.cesm.ucar.edu:/models/cesm2/. Computing and data storage resources, including the Cheyenne supercomputer (https://doi.org/10.5065/D6RX99HX), were provided by the Computational and Information Systems Laboratory (CISL) at NCAR. The CESM datasets used in this study will be made available upon acceptance of the manuscript from the Earth System Grid Federation (ESGF) at esgf-node.llnl.gov/search/cmip6, or from the NCAR Digital Asset Services Hub (DASH) at data.ucar.edu.

References

Bailey DA, Holland MM, DuVivier AK, Hunke EC, Turner AK (2020) Impact of a new sea ice thermodynamic formulation in the CESM2 sea ice component. J Adv Model Earth Syst 12:e2020MS002154. https://doi.org/10.1029/2020MS002154

Baker LH, Collins WJ, Olivié DJL, Cherian R, Hodnebrog Ø, Myhre G, Quaas J (2015) Climate responses to anthropogenic emissions of short-lived climate pollutants. Atmos Chem Phys 15:8201–8216. https://doi.org/10.5194/acp-15-8201-2015

Ban-Weiss GA, Cao L, Bala G, Caldeira K (2012) Dependence of climate forcing and response on the altitude of black carbon aerosols. Clim Dyn 38:897–911. https://doi.org/10.1007/s00382-011-1052-y

Bekkers E, Francois JF, Rojas-Romagosa H (2018) Melting ice caps and the economic impact of opening the Northern sea route. Econ J 128:1095–1127. https://doi.org/10.1111/ecoj.12460

Beljaars ACM, Brown AR, Wood N (2004) A new parametrization of turbulent orographic form drag. Q J R Meteorol Soc 130:1327–1347. https://doi.org/10.1256/qj.03.73

Bond TC et al (2013) Bounding the role of black carbon in the climate system: a scientific assessment. J Geophys Res Atmos 118:5380–5552. https://doi.org/10.1002/jgrd.50171

Briegleb B, Light B (2007) A delta-Eddington multiple scattering parameterization for solar radiation in the sea ice component of the Community Climate System Model NCAR Tech Note NCAR/TN-472+ STR:1–108

Browse J, Carslaw KS, Schmidt A, Corbett JJ (2013) Impact of future Arctic shipping on high-latitude black carbon deposition. Geophys Res Lett 40:4459–4463. https://doi.org/10.1002/grl.50876

Buixadé Farré A et al (2014) Commercial Arctic shipping through the Northeast Passage: routes, resources, governance, technology, and infrastructure. Polar Geogr 37:298–324. https://doi.org/10.1080/1088937X.2014.965769

Chen S, Wu R, Chen W (2019) Projections of climate changes over mid-high latitudes of Eurasia during boreal spring: uncertainty due to internal variability. Clim Dyn 53:6309–6327. https://doi.org/10.1007/s00382-019-04929-4

Cohen J et al (2014) Recent Arctic amplification and extreme mid-latitude weather. Nat Geosci 7:627–637. https://doi.org/10.1038/ngeo2234

Corbett JJ, Lack DA, Winebrake JJ, Harder S, Silberman JA, Gold M (2010) Arctic shipping emissions inventories and future scenarios. Atmos Chem Phys 10:9689–9704. https://doi.org/10.5194/acp-10-9689-2010

Coumou D, Di Capua G, Vavrus S, Wang L, Wang S (2018) The influence of Arctic amplification on mid-latitude summer circulation. Nat Commun 9:2959. https://doi.org/10.1038/s41467-018-05256-8

Danabasoglu G et al (2020) The community earth system model version 2 (CESM2). J Adv Model Earth Syst 12:e2019MS001916. https://doi.org/10.1029/2019ms001916

Deser C, Phillips A, Bourdette V, Teng H (2012) Uncertainty in climate change projections: the role of internal variability. Clim Dyn 38:527–546. https://doi.org/10.1007/s00382-010-0977-x

Deser C et al (2020) Insights from Earth system model initial-condition large ensembles and future prospects. Nat Clim Change 10:277–286. https://doi.org/10.1038/s41558-020-0731-2

DNV G (2020) Initial results of a Black Carbon measurement campaign with emphasis on the impact of the fuel oil quality on Black Carbon emissions. Retrieved from https://www.euractiv.com/wp-content/uploads/sites/2/2020/01/PPR-7-8-Initial-results-of-a-Black-Carbon-measurement-campaign-with-emphasis-on-the-impact-of-the...-Finland-and-Germany.pdf. Accessed 6 Oct 2020

Du Vivier AK, Holland MM, Kay JE, Tilmes S, Gettelman A, Bailey DA (2020) Arctic and Antarctic sea ice mean state in the community earth system model version 2 and the influence of atmospheric chemistry. J Geophys Res Oceans 125:201. https://doi.org/10.1029/2019JC015934

Duarte CM, Lenton TM, Wadhams P, Wassmann P (2012) Abrupt climate change in the Arctic. Nat Clim Change 2:60–62. https://doi.org/10.1038/nclimate1386

Dufresne J-L, Bony S (2008) An assessment of the primary sources of spread of global warming estimates from coupled atmosphere–ocean models. J Clim 21:5135–5144. https://doi.org/10.1175/2008jcli2239.1

Fierce L, Riemer N, Bond TC (2015) Explaining variance in black carbon's aging timescale. Atmos Chem Phys 15:3173–3191. https://doi.org/10.5194/acp-15-3173-2015

Flanner MG (2013) Arctic climate sensitivity to local black carbon. J Geophys Res Atmos 118:1840–1851. https://doi.org/10.1002/jgrd.50176

Flanner MG, Zender CS, Hess PG, Mahowald NM, Painter TH, Ramanathan V, Rasch PJ (2009) Springtime warming and reduced snow cover from carbonaceous particles. Atmos Chem Phys 9:2481–2497. https://doi.org/10.5194/acp-9-2481-2009

Fuglestvedt JS et al (2014) Climate penalty for shifting shipping to the Arctic. Environ Sci Technol 48:13273–13279. https://doi.org/10.1021/es502379d

Gettelman A, Morrison H (2015) Advanced two-moment bulk microphysics for global models part I: off-line tests and comparison with other schemes. J Clim 28:1268–1287. https://doi.org/10.1175/jcli-d-14-00102.1

Gidden MJ et al (2019) Global emissions pathways under different socioeconomic scenarios for use in CMIP6: a dataset of harmonized emissions trajectories through the end of the century. Geosci Model Dev 12:1443–1475. https://doi.org/10.5194/gmd-12-1443-2019

Gillett NP, Fyfe JC (2013) Annular mode changes in the CMIP5 simulations. Geophys Res Lett 40:1189–1193. https://doi.org/10.1002/grl.50249

Golaz J-C, Larson VE, Cotton WR (2002) A PDF-based model for boundary layer clouds part I: method and model description. J Atmos Sci 59:3540–3551. https://doi.org/10.1175/1520-0469(2002)059%3c3540:apbmfb%3e2.0.co;2

Goldstein MA, Lynch AH, Zsom A, Arbetter T, Chang A, Fetterer F (2018) The step-like evolution of arctic open water. Sci Rep 8:16902. https://doi.org/10.1038/s41598-018-35064-5

Grieshop AP, Reynolds CCO, Kandlikar M, Dowlatabadi H (2009) A black-carbon mitigation wedge. Nat Geosci 2:533–534. https://doi.org/10.1038/ngeo595

Gunnarson B (2013) The future of Arctic marine operations and shipping logistics, in the Arctic in World Affairs: a North Pacific Dialogue on the Future of the Arctic. In: Young OR, Kim J-D, Kim YH (eds) Proceedings of the North Pacific Arctic Conference (NPAC). Korea Maritime Institute and East-West Center, Seoul and Honolulu, pp 37–61

Hansen J, Nazarenko L (2004) Soot climate forcing via snow and ice albedos. Proc Natl Acad Sci USA 101:423–428. https://doi.org/10.1073/pnas.2237157100

Hansen CØ, Grønsedt P, Graversen CL, Hendriksen C (2016) Arctic shipping: commercial opportunities and challenges. CBS Maritime, Copenhagen

Haywood J, Boucher O (2000) Estimates of the direct and indirect radiative forcing due to tropospheric aerosols: a review. Rev Geophys 38:513–543. https://doi.org/10.1029/1999RG000078

Hildebrand LP, Brigham LW (2018) Navigating the future: towards sustainable arctic marine operations and shipping in a changing Arctic. In: Hildebrand LP, Brigham LW, Johansson TM (eds) Sustainable shipping in a changing Arctic. Springer International

Publishing, Cham, pp 429–435. https://doi.org/10.1007/978-3-319-78425-0_23
Holland MM, Bailey DA, Briegleb BP, Light B, Hunke E (2012) Improved sea ice shortwave radiation physics in CCSM4: the impact of melt ponds and aerosols on Arctic sea ice. J Clim 25:1413–1430. https://doi.org/10.1175/jcli-d-11-00078.1
Humpert M (2020) IMO moves forward with ban of Arctic HFO but exempts some vessels until 2029. High North News, February 24. https://www.highnorthnews.com/en/imo-moves-forward-ban-arctic-hfo-exempts-some-vessels-until-2029. Accessed 1 Oct 2020
Hunke EC, Hebert DA, Lecomte O (2013) Level-ice melt ponds in the Los Alamos sea ice model. CICE Ocean Model 71:26–42. https://doi.org/10.1016/j.ocemod.2012.11.008
Hunke EC, Lipscomb WH, Turner AK, Jeffery N, Elliott S (2015) CICE: The Los Alamos Sea Ice Model Documentation and Software User's Manual Version 5.1 LA-CC-06-012 T-3 Fluid Dynamics Group, Los Alamos National Laboratory
Johnson BT, Haywood JM, Hawcroft MK (2019) Are changes in atmospheric circulation important for black carbon aerosol impacts on clouds, precipitation, and radiation? J Geophys Res Atmos 124:7930–7950. https://doi.org/10.1029/2019jd030568
Kay JE et al (2015) The community earth system model (CESM) large ensemble project: a community resource for studying climate change in the presence of internal climate variability. Bull Am Meteorol Soc 96:1333–1349. https://doi.org/10.1175/bams-d-13-00255.1
Kwok R (2000) Recent changes in Arctic Ocean sea ice motion associated with the North Atlantic Oscillation. Geophys Res Lett 27:775–778. https://doi.org/10.1029/1999gl002382
Lamarque JF et al (2010) Historical (1850–2000) gridded anthropogenic and biomass burning emissions of reactive gases and aerosols: methodology and application. Atmos Chem Phys 10:7017–7039. https://doi.org/10.5194/acp-10-7017-2010
Lasserre F (2014) Case studies of shipping along Arctic routes. Analysis and profitability perspectives for the container sector. Transp Res Part A Policy Pract 66:144–161. https://doi.org/10.1016/j.tra.2014.05.005
Law KS, Stohl A (2007) Arctic air pollution: origins and impacts. Science 315:1537–1540. https://doi.org/10.1126/science.1137695
Liu X et al (2012) Toward a minimal representation of aerosols in climate models: description and evaluation in the community atmosphere model CAM5. Geosci Model Dev 5:709–739. https://doi.org/10.5194/gmd-5-709-2012
Liu X et al (2016) Description and evaluation of a new four-mode version of the modal aerosol module (MAM4) within version 5.3 of the community atmosphere model. Geosci Model Dev 9:505–522. https://doi.org/10.5194/gmd-9-505-2016
Liu D et al (2020) Efficient vertical transport of black carbon in the planetary boundary layer. Geophys Res Lett 47:e2020GL088858. https://doi.org/10.1029/2020gl088858
Maslanik JA, Lynch AH, Serreze MC, Wu W (2000) A case study of regional climate anomalies in the Arctic: performance requirements for a coupled model. J Clim 13:383–401. https://doi.org/10.1175/1520-0442(2000)013%3c0383:acsorc%3e2.0.co;2
Medeiros B, Deser C, Tomas RA, Kay JE (2011) Arctic inversion strength in climate models. J Clim 24:4733–4740. https://doi.org/10.1175/2011jcli3968.1
Meng Q, Zhang Y, Xu M (2017) Viability of transarctic shipping routes: a literature review from the navigational and commercial perspectives. Marit Policy Manag 44:16–41. https://doi.org/10.1080/03088839.2016.1231428
Miller LB, Hallo JC, Dvorak RG, Fefer JP, Peterson BA (2020) Brownlee MTJ (2020) On the edge of the world: examining pro-environmental outcomes of last chance tourism in Kaktovik, Alaska. J Sustain Tour 10(1080/09669582):1720696
Ng AKY, Andrews J, Babb D, Lin Y, Becker A (2018) Implications of climate change for shipping: opening the Arctic seas WIREs. Clim Change 9:e507. https://doi.org/10.1002/wcc.507
O'Neill BC et al (2014) A new scenario framework for climate change research: the concept of shared socioeconomic pathways. Clim Change 122:387–400. https://doi.org/10.1007/s10584-013-0905-2
Ødemark K, Dalsøren SB, Samset BH, Berntsen TK, Fuglestvedt JS, Myhre G (2012) Short-lived climate forcers from current shipping and petroleum activities in the Arctic. Atmos Chem Phys 12:1979–1993. https://doi.org/10.5194/acp-12-1979-2012
O'Neill BC et al (2016) The scenario model intercomparison project (ScenarioMIP) for CMIP6. Geosci Model Dev 9:3461–3482. https://doi.org/10.5194/gmd-9-3461-2016
Overland JE, Francis JA, Hanna E, Wang M (2012) The recent shift in early summer Arctic atmospheric circulation. Geophys Res Lett. https://doi.org/10.1029/2012gl053268
Parkinson CL, Cavalieri DJ (2008) Arctic sea ice variability and trends, 1979–2006. J Geophys Res Oceans. https://doi.org/10.1029/2007jc004558
Peters GP, Nilssen TB, Lindholt L, Eide MS, Glomsrød S, Eide LI, Fuglestvedt JS (2011) Future emissions from shipping and petroleum activities in the Arctic. Atmos Chem Phys 11:5305–5320. https://doi.org/10.5194/acp-11-5305-2011
Ramanathan V, Carmichael G (2008) Global and regional climate changes due to black carbon. Nat Geosci 1:221–227. https://doi.org/10.1038/ngeo156
Rigor IG, Wallace JM, Colony RL (2002) Response of sea ice to the Arctic Oscillation. J Clim 15:2648–2663. https://doi.org/10.1175/1520-0442(2002)015%3c2648:rositt%3e2.0.co;2
Ryan JC et al (2018) Dark zone of the greenland ice sheet controlled by distributed biologically-active impurities. Nat Commun 9:1065. https://doi.org/10.1038/s41467-018-03353-2
Sand M, Berntsen TK, Kay JE, Lamarque JF, Seland Ø, Kirkevåg A (2013a) The Arctic response to remote and local forcing of black carbon. Atmos Chem Phys 13:211–224. https://doi.org/10.5194/acp-13-211-2013
Sand M, Berntsen TK, Seland Ø, Kristjánsson JE (2013b) Arctic surface temperature change to emissions of black carbon within Arctic or midlatitudes. J Geophys Res Atmos 118:7788–7798. https://doi.org/10.1002/jgrd.50613
Sand M, Berntsen TK, von Salzen K, Flanner MG, Langner J, Victor DG (2016) Response of Arctic temperature to changes in emissions of short-lived climate forcers. Nat Clim Change 6:286–289. https://doi.org/10.1038/nclimate2880
Screen JA, Deser C, Simmonds I, Tomas R (2014) Atmospheric impacts of Arctic sea–ice loss, 1979–2009: separating forced change from atmospheric internal variability. Clim Dyn 43:333–344. https://doi.org/10.1007/s00382-013-1830-9
Shepherd TG (2014) Atmospheric circulation as a source of uncertainty in climate change projections. Nat Geosci 7:703–708. https://doi.org/10.1038/ngeo2253
Shindell DT et al (2008) A multi-model assessment of pollution transport to the Arctic Atmos. Chem Phys 8:5353–5372. https://doi.org/10.5194/acp-8-5353-2008
Reuters Staff (2020) UN approves ban on heavy ship fuel in Arctic. Thomson Reuters, November 20. https://www.reuters.com/article/shipping-arctic-imo/un-approves-ban-on-heavy-ship-fuel-in-arctic-idUKL8N2HY5IS. Accessed 15 Feb 2021
Stephenson SR, Wang W, Zender CS, Wang H, Davis SJ, Rasch PJ (2018) Climatic responses to future trans-Arctic shipping. Geophys Res Lett 45:9898–9908. https://doi.org/10.1029/2018gl078969
Stewart EJ, Howell SEL, Draper D, Yackel J, Tivy A (2007) Sea ice in Canada's Arctic: implications for cruise tourism. Arctic 60:370–380

Stjern CW et al (2017) Rapid adjustments cause weak surface temperature response to increased black carbon concentrations. J Geophys Res Atmos 122:11462–411481. https://doi.org/10.1002/2017jd027326

Theocharis D, Pettit S, Rodrigues VS, Haider J (2018) Arctic shipping: a systematic literature review of comparative studies. J Transp Geogr 69:112–128. https://doi.org/10.1016/j.jtrangeo.2018.04.010

Turner AK, Hunke EC (2015) Impacts of a mushy-layer thermodynamic approach in global sea–ice simulations using the CICE sea–ice model. J Geophys Res Oceans 120:1253–1275. https://doi.org/10.1002/2014JC010358

von Schneidemesser E et al (2015) Chemistry and the linkages between air quality and climate change. Chem Rev 115:3856–3897. https://doi.org/10.1021/acs.chemrev.5b00089

Wan Z, Ge J, Chen J (2018) Energy-saving potential and an economic feasibility analysis for an arctic route between Shanghai and Rotterdam: case Study From China's largest container sea freight. Oper Sustain. https://doi.org/10.3390/su10040921

Wang J et al (2009) Is the dipole anomaly a major driver to record lows in Arctic summer sea ice extent? Geophys Res Lett. https://doi.org/10.1029/2008gl036706

Wang Z, Silberman JA, Corbett JJ (2020) Container vessels diversion pattern to trans-Arctic shipping routes and GHG emission abatement potential. Marit Policy Manag. https://doi.org/10.1080/03088839.2020.1795288

Warren SG (1982) Optical properties of snow. Rev Geophys 20:67–89. https://doi.org/10.1029/RG020i001p00067

Watanabe E, Wang J, Sumi A, Hasumi H (2006) Arctic dipole anomaly and its contribution to sea ice export from the Arctic Ocean in the 20th century. Geophys Res Lett. https://doi.org/10.1029/2006gl028112

Wu D et al (2018) Primary particulate matter emitted from heavy fuel and diesel oil combustion in a typical container ship: characteristics and toxicity. Environ Sci Technol 52:12943–12951. https://doi.org/10.1021/acs.est.8b04471

Yumashev D, van Hussen K, Gille J, Whiteman G (2017) Towards a balanced view of Arctic shipping: estimating economic impacts of emissions from increased traffic on the Northern Sea Route. Clim Change 143:143–155. https://doi.org/10.1007/s10584-017-1980-6